

## Chiral separation in microflows

Marcin Kostur, Michael Schindler, Peter Talkner, Peter Hänggi

*Universität Augsburg, Institut für Physik,  
Universitätsstrasse 1, D-86135 Augsburg, Germany*

corresponding author: Peter Talkner

*Universität Augsburg, Universitätsstrasse 1,  
D-86135 Augsburg, Germany*

*Tel: +49 821 598 3233*

*Fax: +49 821 598 3222*

*peter.talkner@physik.uni-augsburg.de*

x pages, 6 figures, 0 tables

abstract: xxx words, paper: xxxxx characters

(Dated: May 24, 2019)

## Abstract

Molecules that only differ by their chirality, so called enantiomers, often possess different properties with respect to their biological function. Therefore, the separation of enantiomers presents a prominent challenge in molecular biology and belongs to the “Holy Grail” of organic chemistry. We here suggest a new separation technique for chiral molecules that is based on the transport properties in a microfluidic flow with spatially variable vorticity. Because of their size the thermal fluctuating motion of the molecules must be taken into account. These fluctuations play a decisive role in the proposed separation mechanism.

## I. INTRODUCTION

The main established methods of enantiomer separation are gas or liquid chromatography (1) and capillary electrophoresis (2). In both cases suitable and most often specific chiral coating or filling materials are used to obtain different elution times of the enantiomers. Moreover, long columns are needed through which the enantiomers in a solvent are dragged by a large pressure or a high voltage difference. Chemically less specific methods that work with less substance and that in particular do not require high voltages or pressure would be of great advantage.

During the last ten years the development of microfabricated fluid devices mainly designed for biochemical processing has experienced enormous progress (3). For the separation of substances on these so-called labs-on-a-chip the classical methods like electrophoresis have been miniaturized (4, 5) and new ideas how to manipulate small amounts of fluids and substances therein have been suggested (6). Recently, it has been demonstrated that the agitation of fluids by surface acoustic waves on piezoelectric substrates presents a versatile method of manipulating and controlling the flow of small amounts of a fluid both in closed (7) and in open geometries (8).

Various separation mechanisms have been proposed. For example, the separation according to size was predicted for particles in a fluid that is periodically pumped through an array of parallel cylindrical pores with periodically varying ratchet shaped cylinder radius (9, 10). This effect was experimentally corroborated in Ref. 12. A mechanical selection of chiral crystals was suggested by de Gennes (13). He showed that a chiral crystal floating on a liquid surface or gliding on a solid surface under the influence of an external force will in general move in a direction that is different from that of the force and specific for the chirality of the crystal. This suggests a separation method. For molecules, de Gennes argued thermal fluctuations would destroy this effect (13). Here we propose a different mechanism that uses the constructive influence of thermal noise in combination with the nonlinear dynamics of molecules in a flow field in order to attain a separation of opposite chiral partners.

It is well known that a single suspended point-like particle is advectively transported in a flowing viscous fluid. This implies that the particle moves with the instantaneous fluid velocity at the particle's actual position. The corresponding inertial forces are small and can be neglected (14). For an incompressible fluid, the particle motion is volume conserving.

Therefore, the particle trajectories never lose the information on their initial conditions. In particular, this has the consequence that attractors may not exist (17). In two spatial dimensions, the stream function that determines the flow plays the role of an Hamiltonian for the advection dynamics. This dynamics then is integrable with trajectories that coincide with the equipotential lines of the stream function.

For small particles, diffusion provides another transport mechanism, which tends to level out concentration differences of the suspended particles. In the case of a point particle, diffusion in an incompressible arbitrary flow results in a homogeneous distribution if external forces like gravity or electric fields are absent. One also will find a homogeneous particle distribution in three dimensions, in the presence of hydrodynamic interactions between the particles, and for time dependent flows. In all these cases the deterministic dynamics is conservative, i.e. is volume preserving, and the diffusion will lead to an equipartition of point particles.

A qualitatively different picture results for extended particles. Different from the advective motion of a point particle, the local particle velocity at a surface point need not coincide with the fluid velocity that one would observe at this point in the absence of the particle. As a consequence, the volume of the state space spanned by the particle's degrees of freedom is no longer conserved by the dynamics, which, as a result may display attractors if the flow field is stationary, in spite of the fact that the dynamics is reversible (15). In general, several attractors will coexist. Which of them is approached after sufficiently long time depends on the actual initial conditions. If the particle is still small, say with a diameter of  $1 \mu\text{m}$  or less, thermal noise at ambient temperature will have an effect, in particular on the long time dynamics. Constituting a random perturbation of a deterministic motion with multiple attractors the thermal noise will destroy very weak attractors and populate the stronger ones, with weights depending on the stability of the attractors.

We will discuss a minimal model describing this scenario. We restrict ourselves to a two dimensional fluid with a stationary flow characterized by a stream function (16). The extended particle, or “molecule” as we will call it, consists of three spherical “atoms” which are rigidly connected to each other. The action of the fluid on these atoms is given by forces which are proportional to the velocity difference between the fluid at the position of the atom and the atom velocity. The respective friction coefficients are specific for the different atoms of the molecule. In this way we can model *chiral* molecules for example by

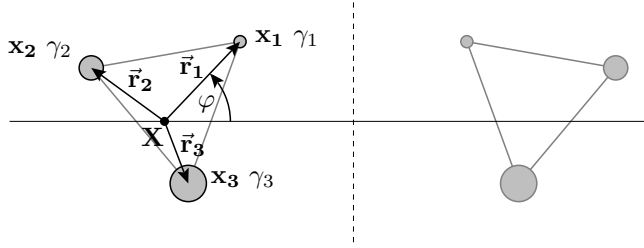


FIG. 1: A molecule consisting of three atoms at positions  $\mathbf{x}_i = \mathbf{X} + \mathbf{r}_i$  with different friction coefficients  $\gamma_i$  and its chiral partner. The angle  $\varphi$  describes the position relative to a reference configuration with the same center of friction  $X$ . The rigid rods are indicated by gray lines connecting the atoms.

choosing the corners of an equilateral triangle as the atoms' positions and giving the friction coefficients three different values. The mirror image of such a molecule does not match with the original molecule upon any combination of translations and rotations in the plane. It is the dependence of the transport properties on the chirality which is in the focus of this paper. Locally, the differences between the dynamics of chiral partners possibly are rather small but for the asymptotic dynamics at long times they will lead to different attractors with different stability properties. With the omnipresence of thermal noise in the fluid these different stability patterns will cause spatial distributions that are different for chiral partners to an extent that they can be used for an effective chiral separation.

## II. THE MOTION OF AN EXTENDED MOLECULE IN A FLOWING FLUID

We consider three atoms with positions  $\mathbf{x}_i$ ,  $i = 1, 2, 3$  that are mutually connected by rigid rods, see Fig. 1. The force on the  $i$ -th particle exerted by the fluid moving with velocity  $\mathbf{v}(\mathbf{x})$  is assumed to be proportional to the relative velocity of the particle with respect to that of the fluid, i.e.,

$$\mathbf{F}_i^{\text{fl}} = \gamma_i (\mathbf{v}(\mathbf{x}_i) - \dot{\mathbf{x}}_i) \quad [1]$$

where  $\gamma_i$  denotes the friction coefficient of the  $i$ -th atom,  $\dot{\mathbf{x}}_i$  is the instantaneous velocity of the  $i$ th particle, and  $\mathbf{v}(\mathbf{x})$  is the velocity field of the fluid in absence of the atoms. In a fluid at temperature  $T$ , the frictional forces are always accompanied by random forces, which, for the sake of simplicity, are assumed to be independent Gaussian thermal white noises  $\boldsymbol{\xi}_i(t)$  with independent cartesian components  $\xi_{i,\alpha}(t)$ ,  $\alpha = 1, 2$ , satisfying the fluctuation-dissipation

relation

$$\begin{aligned}\langle \boldsymbol{\xi}_i(t) \rangle &= 0, \\ \langle \xi_{i,\alpha}(t) \xi_{j,\beta}(s) \rangle &= \gamma_i k_B T \delta_{i,j} \delta_{\alpha,\beta} \delta(t-s).\end{aligned}\quad [2]$$

We also have to take into account forces  $\mathbf{F}_{i,j}$  caused by the  $j$ -th atom and acting on the  $i$ -th atom that maintain the rigid structure of the molecule. In our model these forces are provided by rigid rods. They obey Newton's *actio = reactio* principle and may not impose any torque on the molecule. For the minimal model considered here, we neglect hydrodynamic interactions between the individual atoms (18).

In order to properly account for the constraints we use d'Alembert's principle

$$\sum_i \left\{ \gamma_i [\mathbf{v}(\mathbf{x}_i) - \dot{\mathbf{x}}_i] + \sum_{j \neq i} \mathbf{F}_{i,j} + \boldsymbol{\xi}_i(t) \right\} \cdot \delta \mathbf{x}_i = 0 \quad [3]$$

where  $\delta \mathbf{x}_i$  are virtual displacements which conform to the constraints. Here, we neglected inertial terms which are extremely small and of short duration for small suspended particles (14). The allowed displacements are translations of the molecule as a whole, and rigid rotations. It is convenient to specify the momentary position of the molecule by means of the center of friction  $\mathbf{X}$  which is analogously defined as the center of gravity with the masses replaced by the respective friction coefficients, i.e.,

$$\mathbf{X} = \sum_i \frac{\gamma_i}{\sum_j \gamma_j} \mathbf{x}_i, \quad [4]$$

and by an angle  $\varphi$  fixing the orientation, see Fig. 1. The position of the atoms can then be recovered as

$$\mathbf{x}_i = \mathbf{X} + \mathbf{r}_i(\varphi) \quad [5]$$

where the vector  $\mathbf{r}_i(\varphi)$  pointing from the center of friction to the  $i$ -th atom results from a reference configuration  $\mathbf{r}_i^{(0)}$  by the rotation with the angle  $\varphi$

$$\mathbf{r}_i(\varphi) = \mathbb{R}(\varphi) \mathbf{r}_i^{(0)}. \quad [6]$$

Here,  $\mathbb{R}(\varphi)$  denotes the rotation matrix

$$\mathbb{R}(\varphi) = \begin{pmatrix} \cos(\varphi) & -\sin(\varphi) \\ \sin(\varphi) & \cos(\varphi) \end{pmatrix}. \quad [7]$$

Choosing translations ( $\delta \mathbf{x}_i = \delta \mathbf{X}$ ) and rotations ( $\delta \mathbf{x}_i = \mathbf{r}'_i(\varphi)\delta\varphi$ ) separately as displacements, we obtain coupled equations of motion for the center of friction and the angle  $\varphi$  that no longer contain the constraint forces

$$\dot{\mathbf{X}} = \sum_i \frac{\gamma_i}{\sum_j \gamma_j} \mathbf{v}(\mathbf{X} + \mathbf{r}_i(\varphi)) + \boldsymbol{\xi}_{\mathbf{X}}, \quad [8]$$

$$\dot{\varphi} = \sum_i \frac{\gamma_i}{\sum_j \gamma_j \mathbf{r}_j^2} \mathbf{r}'_i(\varphi) \cdot \mathbf{v}(\mathbf{X} + \mathbf{r}_i(\varphi)) + \xi_\varphi \quad [9]$$

where a dot denotes a time derivative and the prime a derivative with respect to the angle  $\varphi$ . Note that the second moment  $\sum \gamma_i \mathbf{r}_i^2$  is independent of  $\varphi$  and, hence, represents an invariant property of the molecule. The fluctuating forces  $\boldsymbol{\xi}_{\mathbf{X}}(t)$  and  $\xi_\varphi(t)$  are linear combinations of the original ones, reading

$$\boldsymbol{\xi}_{\mathbf{X}} = \frac{1}{\sum_i \gamma_i} \sum_i \boldsymbol{\xi}_i, \quad [10]$$

$$\xi_\varphi = \frac{1}{\sum_i \gamma_i \mathbf{r}_i^2} \sum_i \mathbf{r}'_i(\varphi) \cdot \boldsymbol{\xi}_i. \quad [11]$$

They are also Gaussian and hence characterized by their moments and correlation functions following from eq. 2

$$\langle \xi_{\mathbf{X}\alpha}(t) \xi_{\mathbf{X}\beta}(s) \rangle = 2 \frac{k_B T}{\sum_i \gamma_i} \delta_{\alpha,\beta} \delta(t-s), \quad [12]$$

$$\langle \xi_{\mathbf{X}\alpha}(t) \xi_\varphi(s) \rangle = 0, \quad [13]$$

$$\langle \xi_\varphi(t) \xi_\varphi(s) \rangle = 2 \frac{k_B T}{\sum_i \gamma_i \mathbf{r}_i^2} \delta(t-s). \quad [14]$$

The last equation exhibits that the seeming dependence of  $\xi_\varphi$  on  $\varphi$  in eq. 11 is spurious. Hence, the motions of the center of friction and of the angle are governed by Langevin equations with three independent additive random forces.

### III. DETERMINISTIC TRANSPORT

In a first step, we disregard the fluctuating forces  $\xi_{\mathbf{X}}$  and  $\xi_{\varphi}$  in the eqs. **8** and **9** and discuss the deterministic transport properties. First, we note that the advective dynamics is recovered if the change of velocity over the size of a molecule can be neglected as compared to the velocity itself, i.e. under the condition  $\max \|\mathbf{v}(\mathbf{X} + \mathbf{r}_i(\varphi)) - \mathbf{v}(\mathbf{X})\| \ll \|\mathbf{v}(\mathbf{X})\|$  where the maximum has to be taken with respect to  $i = 1, 2, 3$  and to  $\varphi \in [0, 2\pi]$ , with  $\|\mathbf{v}\|$  denoting the length of the vector  $\mathbf{v}$ . In this small particle limit eq. **8** simplifies to read

$$\dot{\mathbf{X}} = \mathbf{v}(\mathbf{X}). \quad [15]$$

The molecule also performs an angular motion, which, in the small particle limit, is given by

$$\dot{\varphi} = \sum_i \frac{\gamma_i}{\sum_j \gamma_j \mathbf{r}_j^2} r'_{i,\alpha}(\varphi) r_{i,\beta}(\varphi) \frac{\partial v_{\alpha}(\mathbf{X})}{\partial X_{\beta}}, \quad [16]$$

where a sum over the double Greek indices is understood. In the small particle limit the coupling between the motions of the center of friction and of the orientation is unidirectional. The orientation of the molecule does not influence the motion of its center of friction. Thus no separation scenario is possible.

For finite particles, however, the angular motion acts back onto the motion of the center of friction. In distinct contrast to the two-dimensional velocity field, the three-dimensional vector field that governs the coupled motion in general has a non-vanishing divergence. It is therefore possible that the long-time dynamics is governed by one or more attractors which are approached from different initial conditions. The resulting structure of the state space being spanned by  $\mathbf{X}$  and  $\varphi$  though will depend on the properties of the molecule and on the considered velocity field  $\mathbf{v}(\mathbf{x})$ .

### IV. THE VELOCITY FIELD

The velocity field of an incompressible two dimensional fluid can always be expressed in terms of a scalar stream function  $\Psi(x, y)$ . For the sake of definiteness we here choose

$$\Psi(x, y) = V_0 L_0 \frac{\sin(\pi x/L_0) \sin(\pi y/L_0)}{(2 - \cos(\pi x/L_0))(3 - 2 \cos(\pi y/L_0))}. \quad [17]$$

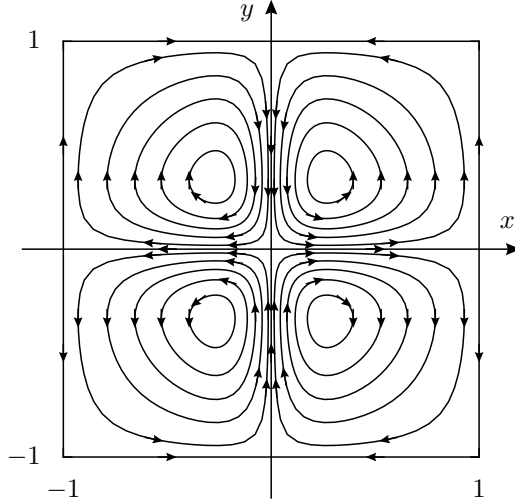


FIG. 2: The stream function given by eq. 17 is shown in one unit cell. The streamlines circulate around the extrema in the counterclockwise direction in the right upper and in the left lower quarter and in the clockwise direction in the remaining two quarters. At points with integer coordinates the stream function has saddle points.

This is a periodic function with period length  $2L_0$  in both  $x$  and  $y$  direction; the velocity scale is determined by  $V_0$ . Here we use dimensionless variables for which  $L_0 = 1$  and  $V_0 = \sqrt{15}$  leading to a root mean square velocity which is approximately one. Within a unit cell, say for  $x \in [-1, 1]$  and  $y \in [-1, 1]$ , the stream function possesses four extrema, one per quadrant, and thus gives rise to four eddies, see in Fig. 2. Apart from the periodic symmetry,

$$\Psi(x + 2, y) = \Psi(x, y + 2) = \Psi(x, y), \quad [18]$$

the stream function transforms oddly under reflections at the coordinate axes:

$$\Psi(x, -y) = \Psi(-x, y) = -\Psi(x, y). \quad [19]$$

The straight lines  $x = 0, \pm 1$ , and  $y = 0, \pm 1$  are the principle axes of four saddle points of the stream function within the unit cell. They make up the boundaries of four invariant regions within the unit cell which will be referred to as quarters in the following. Within each quarter, the streamlines are closed curves which revolve around an extremum of the stream function. The velocity field follows from the stream function as

$$v_x(\mathbf{x}) = \frac{\partial \Psi(\mathbf{x})}{\partial y}, \quad v_y(\mathbf{x}) = -\frac{\partial \Psi(\mathbf{x})}{\partial x}. \quad [20]$$

This velocity field is the solution of the Stokes equation (16)

$$\mu\Delta\mathbf{v}(\mathbf{x}) - \nabla p(\mathbf{x}) = -\mathbf{f}(\mathbf{x}), \quad [21]$$

$$\nabla \cdot \mathbf{v}(\mathbf{x}) = 0 \quad [22]$$

where  $\mu$  denotes the viscosity of the fluid,  $p(\mathbf{x})$  the pressure and  $\mathbf{f}(\mathbf{x})$  a force density with quadrupolar symmetry which we do not specify here because it is a quite involved expression. This force density could be generated by properly shaped interdigital transducers on a piezoelectric substrate emanating surface acoustic waves (7). Even simpler dipolar force densities generate similar streaming patterns of the same quadrupolar symmetry but the analytic form of the resulting stream function is more complicated than the one given by eq. 17, see in Ref. 7.

The advective transport, which is determined by eq. 15, follows the streamlines. It is therefore confined to either of the quarters within the unit cell. To each quarter, a definite parity can be assigned according to the clockwise or anticlockwise circulation of the streamlines.

## V. DETERMINISTIC TRANSPORT OF FINITE PARTICLES

As mentioned above, the motion of finite, but still small, particles is qualitatively different from the advective motion of point particles. The dynamics in the three-dimensional state space spanned by the two translational and one orientational degrees of freedom is no longer conservative. It can be partitioned into different domains of attraction. The detailed structure of the attractors and of their corresponding domains of attraction depends on the size of the molecule, on the magnitude of the friction coefficients and also on their sequence and therefore on the chirality of the molecule. For a pair of enantiomers Fig. 3 depicts cuts of the domains of attraction at a fixed orientation  $\varphi$  and the corresponding attractors whose projections onto the plane of translational degrees of freedom are located within the upper right quarter of the unit cell. In the particular case shown in Fig. 3, there exist three such attractors for one enantiomer, two of which have period one, i.e. after one full rotation of  $\varphi$  the molecule's center of friction has returned to its initial position. The third attractor is chaotic. In contrast, the respective chiral partner has four attractors in this quarter.

Three of them are similar to the attractors of the first enantiomer: The chaotic attractor and one of the period-one attractors still exists; the other period-one attractor is replaced by an attractor with winding number  $42/43$ , i.e. after 42 full rotations of the orientation  $\varphi$  and, simultaneously, after 43 revolutions of the center of friction the molecule has regained its initial position. The fourth attractor is periodic. Here, the orientation  $\varphi$  performs a libration and the translational degrees of freedom move in relatively close distance from the boundary of the considered quarter. This attractor and also the chaotic attractor “collects” also points from adjacent quarters, see the left panel of the bottom row in Fig. 3. In contrast, for the chiral partner only a very small set of points from outside the considered quarter is attracted, see the left panel of the top row in Fig. 3.

For smaller molecules also more complicated trajectories exist that stay close to the boundaries of several quarters. However, also these trajectories differ for opposite chiral partners and populate preferentially quarters with a parity that is specific for the chirality of the molecule. As a consequence, if a swarm of molecules starts at the point of highest symmetry of the velocity field with an uniform distribution of orientations, the particles will become unequally distributed into the quarters with different parity, see Fig 4. In two dimensions, this may provide an effective method of enantiomer separation.

## VI. INFLUENCE OF NOISE

According to their different positions and geometrical structures, the attractors of unlike enantiomers will have different strengths within a quarter of definite parity, and consequently will differ in stability with respect to thermal noise. At a sufficiently low noise level almost all molecules will settle into the attractor with highest stability, provided the system is given sufficient time to relax into its stationary state. This gives rise to unequal distributions of molecules of different chirality in quarters of different parity, see Fig 5. For the transport of a molecule from a quarter with the “wrong” to one with the fitting parity the attractors close to the quarters’ boundaries, like the red one in Fig. 3, may act as a turnstile.

Because transitions from any less stable to the most stable attractor will become increasingly rare with decreasing noise, the time to approach the stationary state may emerge as very long. On the other hand, with higher noise levels “wrong” attractors will be populated with increasing probability and therefore the separation quality deteriorates. In Fig. 6 the

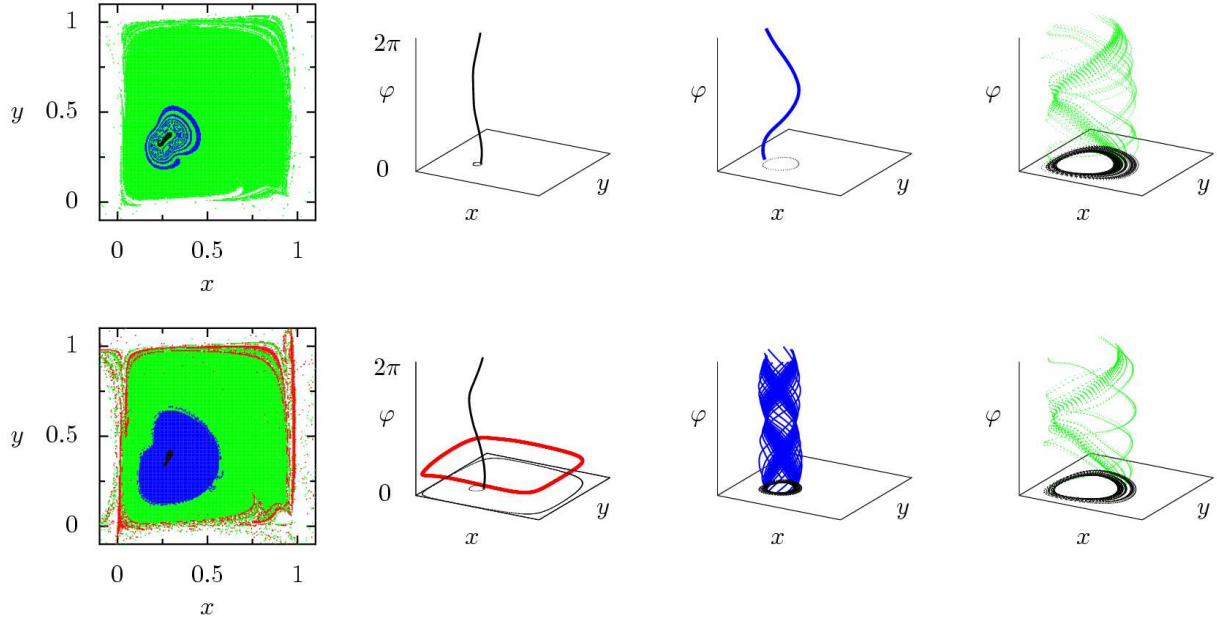


FIG. 3: In the top row the deterministic motion of an equilateral molecule resulting from eqs. **8**, **9** with the velocity field **17**, **20** is visualized. The left panel shows a cut through the domains of attraction at  $\varphi = 2$  of those attractors which are located within the upper right quarter of the unit cell, ( see Fig. 2). The molecule's side length is  $d = 0.2$  and its friction constants are  $(\gamma_1, \gamma_2, \gamma_3) = (1/6, 1/3, 1/2)$ . The other three panels of the top row depict the corresponding attractors in the full state space. The domains of attraction and the respective attractors are indicated by the same color. Trajectories starting from the white regions do not approach the displayed quarter. In the bottom row, the corresponding information is displayed for the chiral partner molecule with friction coefficients  $(\gamma_1, \gamma_2, \gamma_3) = (1/3, 1/6, 1/2)$ . Note that the domain of attraction of the additional red attractor extends beyond the upper right quarter and consequently attracts trajectories starting outside of this quarter.

time to reach the stationary state and the separation performance are compared as they vary with the noise strength. The noise strength is quantified by the dimensionless quantity  $k_B T / \sum_i \gamma_i L_0 V_0$ . It is therefore not only determined by the temperature but also by the total friction, as well as by the characteristic eddy size and the velocity scale.

## VII. CONCLUSIONS

We elucidated the transport properties of a chiral extended object in a two-dimensional model flow in view of enantiomer separation. We examined two methods: The first one is based on the asymmetric distribution of different chiral partners that results in the absence of noise when a racemic mixture is injected into the region of highest symmetry of the

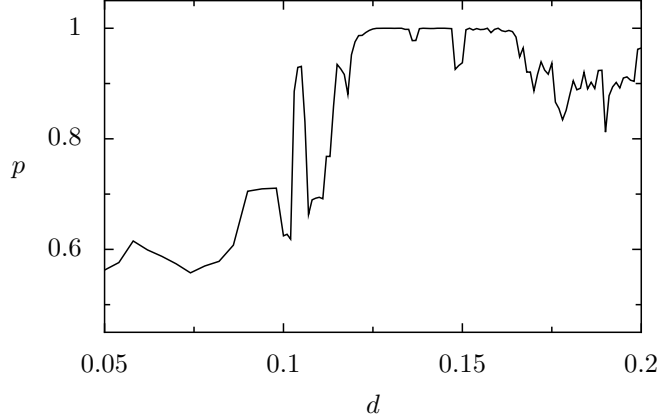


FIG. 4: The injection of a racemic mixture into the point of highest symmetry leads to an unequal distribution of chiral partners within quarters of different parity. In this figure the fraction  $p = N_+/(N_+ + N_-)$  of the number  $N_+$  of molecules with friction coefficients  $(\gamma_1, \gamma_2, \gamma_3) = (1/6, 1/3, 1/2)$  and the total number of molecules within all quarters with clockwise parity is displayed as a function of the side length  $d$  of equilateral molecules.

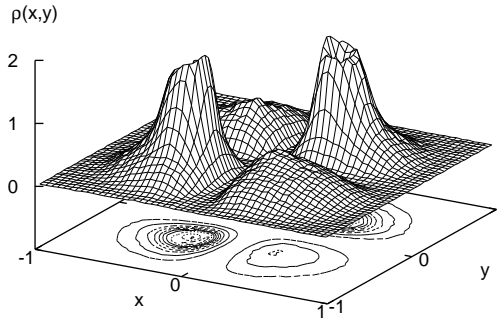


FIG. 5: For a single chiral molecule with size  $d = 0.2$  the stationary probability density integrated over all orientations  $\varphi$  exhibits a pronounced asymmetry with respect to quarters of different parity. The friction coefficients are the same as in Fig. 4 and the dimensionless noise strength is  $k_B T / \sum_i \gamma_i L_0 V_0 = 10^{-3}$ .

velocity field. This method is sensitive to unavoidable asymmetries of the initial distribution. There is no deterministic mechanism that would compensate for such a bias. Notably, the trajectories of too small particles will stay very close to the quarter boundaries and therefore the separation would be difficult from a practical point of view. These drawbacks can be avoided by the second method. Here, one starts from a uniform distribution of the racemic mixture and waits until the combined action of the advective transport and of the thermal fluctuations has led to a stationary distribution. In this stationary state, quarters with

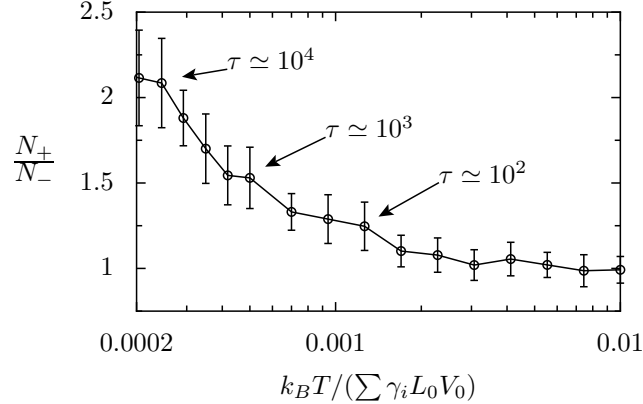


FIG. 6: The selectivity as given by the fraction of numbers of molecules with different chirality  $N_+/N_-$  in a quarter of definite parity decreases as the dimensionless noise strength  $k_B T / \sum \gamma_i L_0 V_0$  increases. The time it needs to reach the stationary value is indicated in units of  $L_0/V_0$  for three different values of the noise strength. It dramatically increases with decreasing noise strength. For the parameters of the molecule see Fig. 3. The error bars indicate the variance as it results from the numerical estimate.

different parity will contain different amounts of a specific enantiomer.

We are convinced that the same mechanisms will also work in a three dimensional helical flow again leading to enantiomer separation. To generate the necessary helical flow patterns in microfluidic devices may though be a difficult experimental problem. Alternatively, one could use the previously developed technique of producing flow patterns between two parallel plates by means of surface acoustic waves (7). The symmetry between the upper and the lower plates could be broken by means of an electric field perpendicular to the plates.

There are several aspects already in two dimensions which we have not addressed with this first investigation. In particular, the model of a molecule consisting of pointlike atoms rigidly connected by rods, which do not interact with the flow, presents a basic working setup that can be approved to account for more complex situations. Future work will have to consider as well more realistic boundary conditions. However, it is clear that our simple model does capture the relevant aspects of symmetry and of the stochastic dynamics of small but extended particles. We are sure that these very aspects will also lead to chiral separation for more realistic models describing e.g. spatially extended atoms, hydrodynamic interactions between them, as well as flexible bonds.

## Acknowledgments

Financial support by the Deutsche Forschungsgemeinschaft via the grant 1517/25-1 and SFB 486 is gratefully acknowledged.

---

1. Ahuja S. (2002) *Chromatography and Separation Science* (Academic Press, New York).
2. Fujimoto C. (2002) *Anal. Sci.* **18**, 19-25.
3. Figeys D. & Pinto D. (2000) *Analytical Chemistry* **72**, 330A-335A.
4. Bruin G. J. M. (2000) *Electrophoresis* **21**, 3931-3951.
5. Tegenfeldt J. O., Prinz C., Cao H., Huang R. L., Austin R. H., Chou S. Y., Cox E. C. & Sturm J. C. (2004) *Analytical and Bioanalytical Chemistry* **378**, 1678-1692.
6. Stone H. A., Stroock A. D. & Ajdari A. (2004) *Annu. Rev. Fluid. Mech.* **36** 381-411.
7. Guttenberg Z., Rathgeber A., Keller S., Rädler J. O., Wixforth A., Kostur M., Schindler M. & Talkner P. (2004) *Phys. Rev. E* **70**, 056311.
8. Guttenberg Z., Müller H., Habermüller H., Geisbauer A., Pipper J., Felbel J., Kielpinski M., Scriba J. & Wixforth A. (2005) *Lab on a Chip* **5**, 308-317.
9. Kettner C., Reimann P., Hänggi P. & Müller F. (2000) *Phys. Rev. E* **61**, 312-323.
10. Astumian R. D. & Hänggi P. (2002) *Physics Today* **55** no.11, 33-39.
11. Hänggi P., Marchesoni F. & Nori F. (2005) *Ann. Phys. (Leipzig)* **14**, 51-70.
12. Matthias S. & Müller F. (2003) *Nature* **424**, 53-57.
13. de Gennes P. G. (1999) *Europhys. Lett.* **46**, 827-830.
14. Purcell E. M. (1977) *Am. J. Phys.* **45**, 3-11.
15. Politi A., Oppo G. L. & Badii R. (1986) *Phys. Rev. E* **33**, 4055-4060.
16. Batchelor G. K. (1967) *Fluid Dynamics* (Cambridge University Press, Cambridge).
17. Lichtenberg A. J., Liebermann M. A. (1992) *Regular and Chaotic Dynamics* (Springer Verlag, Berlin).
18. Dhont J. K. G. (1996) *An Introduction to Dynamics of Colloids* (Elsevier, Amsterdam).